Construction and Building Materials 368 (2023) 130461

Contents lists available at ScienceDirect

Construction and Building Materials

journal homepage: www.elsevier.com/locate/conbuildmat

On the porosity of low-clinker shotcrete and accelerated pastes

Florian R. Steindl [a,b,*], Florian Mittermayr [b], Marlene Sakoparnig [b], Joachim Juhart [b], Lukas Briendl [b], Benedikt Lindlar [c], Neven Ukrainczyk [d], Martin Dietzel [a], Wolfgang Kusterle [e], Isabel Galan [a]

[a] Graz University of Technology and NAWI Graz Geocenter, Institute of Applied Geosciences, Rechbauerstrasse 12, 8010 Graz, Austria
[b] Graz University of Technology, Institute of Technology and Testing of Building Materials, Inffeldgasse 24, 8010 Graz, Austria
[c] Sika Services AG, Tüffenwies 16, 8048 Zurich, Switzerland
[d] Technical University of Darmstadt, Institute of Construction and Building Materials, Franziska-Braun-Strasse 3, 64287 Darmstadt, Germany
[e] OTH Regensburg, Concrete Laboratory, Galgenbergstrasse 30, 93053 Regensburg, Germany

ARTICLE INFO

Keywords:
Porosity
Shotcrete
Mercury Intrusion
Durability
SCMs

ABSTRACT

Although the number and size of interconnected pores have been identified as the most important aspects of concrete microstructure, comprehensive datasets on shotcrete porosity and pore size distributions are still scarce and their key controls are poorly investigated. In this study we investigate the effects of the spraying process, setting accelerator addition and mix design on the microstructure of real-scale dry- and wet-mix shotcrete and hand-mixed and sprayed accelerated pastes. A newly proposed deconvolution analysis of the pore size distributions, measured by mercury intrusion porosimetry, offers increased precision in determining the critical and median pore diameter parameters. In total >50 samples were analysed. Results show that the dry-mix shotcrete exhibits a shift towards coarser pore sizes (~100–1 μm) than wet-mix shotcrete. Combinations of different supplementary cementitious materials are favourable for producing wet-mix shotcretes with refined pore structures. The addition of setting accelerators, up to 10 wt-% of binder mass, and the spraying process cause systematic variations in the pore volume and pore structure of (sprayed) paste and shotcrete.

1. Introduction

Cement-based materials are porous across a wide range of pore sizes. Pores in concrete matrices are, albeit not entirely consistently throughout the literature, roughly classified according to their size into gel pores (typically < 10 nm), capillary pores (10 nm-10 μm) and entrained/entrapped air voids (>10 μm) [1–5]. The permeability, compressive strength and diffusivity of porous materials are heavily influenced by the pore size distribution, pore structure and pore interconnectivity.

A range of instrumental methods exists in cement and concrete research to characterise these parameters, like isothermal gas adsorption (BET, BJH), X-ray computer tomography (CT), image analysis, water absorption, or mercury intrusion porosimetry (MIP). The former methods only measure a limited range of pore diameters, < 200 nm for BJH and > 60 nm, but typically > 1 μm, for CT [4,6]. For image analysis, the range of pore diameters is limited by the resolution of the optical or electron microscope used. (Boiled) water absorption tests (*e.g.* in EN 1936, ASTM C642 or NF P18–459), which are sometimes recommended for shotcrete, do not provide information on the pore size distribution and may in some cases alter the sample due to high drying temperatures > 100 °C. Boiled water absorption has also been critisised by some researchers as a poor permeability indicator for concrete and shotcrete [7,8]. In addition, the comparability of all these methods is limited by the varying resolution and measuring ranges. On the other hand, MIP is able to measure across a wide range of pore diameters of several 100 μm to 4 nm [9] with relatively little effort and expense compared to *e.g.* synchrotron X-ray CT or image analysis with electron microscopes.

Despite physical limitations of the MIP technique, like the so-called ink-bottle effect, and assumptions taken for the data processing, like the shape of the pores [9,10], it is nowadays widely accepted that the total intruded pore volume and the critical pore size are relatively unaffected by the aforementioned limitations and can be derived through MIP. The critical pore size (given as *e.g.* critical pore diameter, CPD) is the mode of the pore size distribution and as such marks the point of the steepest slope of the cumulative intrusion curve [11]. Other important

* Corresponding author.
E-mail address: florian.steindl@tugraz.at (F.R. Steindl).

https://doi.org/10.1016/j.conbuildmat.2023.130461
Received 17 August 2022; Received in revised form 3 December 2022; Accepted 17 January 2023
Available online 28 January 2023

distribution parameters are, for example, the average and median pore size. The deduction of these parameters, especially the critical and median pore diameter, from the measured data involves a certain amount of processing (for example numerical derivation). Depending on the level of scatter in the measured data and the subsequent application of data smoothing, these processing steps can result in significant errors, especially if the parameters are determined automatically by software. This study proposes a new method to characterise pore size distribution curves based on a multi-peak deconvolution analysis.

As mentioned, the number, size and connectivity of the pores in concrete heavily influence the pore volume, permeability and diffusivity of the material and thus its strength and durability properties. This is especially important in challenging environments where the concrete is in direct contact with the surrounding rock and percolating ground waters. In particular, tunnels, river walls, caverns or other underground structures are often built using shotcrete due to its application versatility and fast-setting properties. In these structures exposure to *e.g.* carbonation or chemically aggressive solutions can cause considerable durability declines [12,13].

Shotcrete is produced by spraying a mixture of aggregates, cementitious materials and water onto a receiving substrate such as a rock face in tunneling. Depending on regional and construction specifics, the shotcrete can either be applied in the dry-mix or the wet-mix process [14]. For dry-mix shotcrete, water is added to a dry mix (*i.e.* cement, aggregates, additions and solid admixtures) at the spraying nozzle (Fig. 1). For wet-mix shotcrete, ready-mix concrete (water, cement, aggregates, additions and admixtures) is produced and pumped to the nozzle where it gets intermixed with the setting accelerator and consequently sprayed with pressurised air [15] (Fig. 2). Due to the use of accelerator and/or special binders and the spraying process itself, the chemical and structural properties of shotcrete markedly differ from those of cast concrete [16–21]. Additionally, the cement used for shotcrete is being increasingly substituted with supplementary cementitious materials (SCMs) to improve the durability performance and to decrease the environmental impact such as carbon footprint [22].

All these factors potentially have strong influences on the porosity and pore structure. However, recent studies on the porosity of modern shotcretes are still scarce, although some researchers suppose that porosity influences the durability of shotcrete more than that of cast concrete [23]. Some recent studies have determined the water-accessible porosity of shotcrete [18,24], but have not made use of MIP to characterize the pore size distribution. MIP on shotcrete samples has previously been used, for example, to study high-temperature changes in shotcrete porosity [25,26], to validate the impact of fly ash additions and water/binder variations [27], to investigate the influence of different setting accelerators on the microstructure of sprayed pastes [28], or to characterize the effect of curing temperature or nanoparticles on the microstructure of accelerated concrete [29,30].

To date no comprehensive datasets on shotcrete porosity and pores size distribution have been compiled. The influence of variations in the mix design, such as varying binder compositions or the dosage of setting accelerators or air entrainers, is not well understood in comparison to "normal" cast concrete despite the obvious physical and chemical differences of shotcrete. In this study, we applied MIP on a large set of 10 dry-mix and 17 wet-mix shotcrete samples produced in real-scale spraying tests and one ready-mix concrete sample to investigate the influence of variations in the binder composition and application method. This data set is complemented with 12 hand-mixed and 9 sprayed paste samples (produced at lab-scale without aggregates). In total >50 samples were investigated by the above mentioned deconvolution method. The results show significant influences of SCM addition, the setting accelerator and the spraying process on shotcrete porosity.

2. Materials, testing procedures, and methods

2.1. Real-scale shotcrete mix design and fabrication

2.1.1. Dry-mix shotcrete

A set of dry-mix shotcretes with 10 different mix designs was formulated and samples were fabricated in spray tests (see also [31,32] and Fig. 1). For each mix 300 kg of dry-mix were produced by premixing the binder (cement + SCMs) with carbonate aggregates (grain size 0–8 mm, see Supplementary Fig. 1) (see Table 1 for the mix designs and Table 2 for the binder compositions). The cements used were a spray cement (SpC) as classified according to the Austrian Sprayed Concrete Guidelines [33], two calcium-aluminate cements (CAC1 and 2), and a CEM I 52.5 N SR0 (Type V portland cement according to ASTM C 150), from now on called CEM I SR0 1. The additions (SCMs) consisted of ground blast-furnace slag (GBFS), fine calcium carbonate (FCC2) and metakaolin (MK).

The mixes were sprayed onto spray panels with an Aliva 246 dry-mix shotcrete machine and a Schuller S-2 nozzle at a flow rate of 2.5 $m^3\,h^{-1}$. D3 was the only mix where the addition of a solid setting accelerator (SA1) was necessary, as the used binder of all other mixes was rapid-setting by itself. For D9 and D10, a rebound-reducer (RR) and/or a PCE-based superplasticiser (SP-PCE1) were added at the nozzle. The water/binder (w/b) ratio (0.49 ± 0.11) of each mix was adjusted by the nozzleman to achieve sufficient workability, and was later calculated from the amount of water measured by a flow meter. After a curing time of one day, drill cores with a diameter of 100 mm were taken from the panels (avoiding the panel walls by at least several cm) and stored under tap water for 90 days.

2.1.2. Wet-mix shotcrete

A set of wet-mix shotcretes with 18 mix designs was fabricated in three real-scale spraying tests (W1-W8, W9-13, W14-W18) (see also Fig. 2). Data on mixes W1-W8 has also been presented in [34]. All mixes were sprayed with comparable spraying equipment (Hittmayr-Cifa, Meyco or Sika) and double piston concrete pumps. $Al_2(SO_4)_3$-based alkali-free setting accelerators (SA2, SA3, SA4; see Supplementary Table 2 for detailed properties) were added using squeeze rotor hose (peristaltic) pumps. More information on the chemistry and function of such setting accelerators can be found in appropriate literature, *e.g.* [15,16,35,36]. The mix W17 was not sprayed but cast, hence no setting

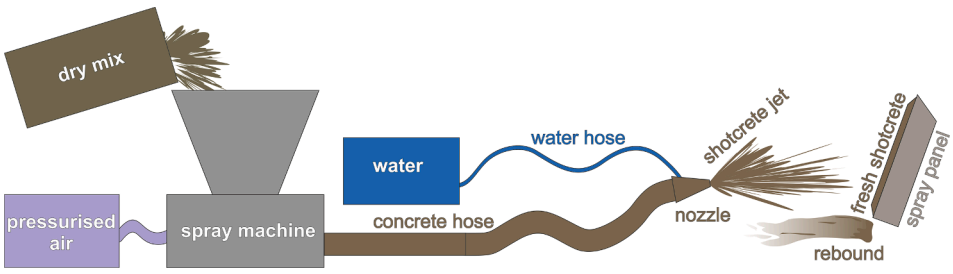

Fig. 1. Schematic diagram of the dry-mix shotcrete process as used for this study. Notice the absence of an accelerator hose due to the fast-setting properties of the spray binder (see text for further explanations).

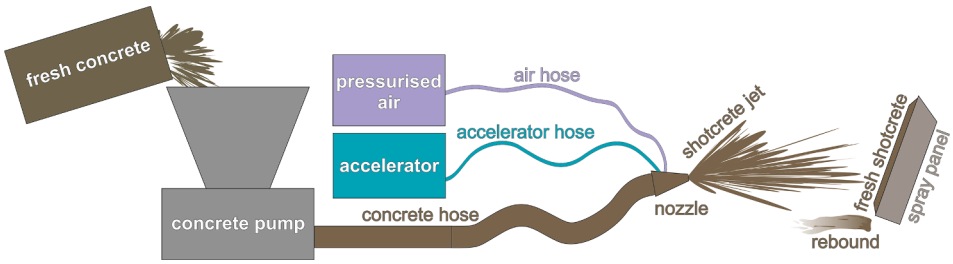

Fig. 2. Schematic diagram of the wet-mix shotcrete process as used for this study. In this setup, the liquid accelerator is added at the nozzle (see text for further explanations).

Table 1
Mix design of the dry-mix shotcrete recipes under investigation.

Mix. No	Aggregates	Binder	Water	w/b	SA	Admixtures
	kg m^{-3}			–	wt-% relativ to binder	
D1	1843	347	209	0.60	–	–
D2	1918	361	178	0.49	–	–
D3	1944	364	172	0.47	3.1% SA1	–
D4	1935	361	177	0.49	–	–
D5	1943	365	170	0.47	–	–
D6	1982	374	151	0.41	–	–
D7	1941	366	166	0.45	–	–
D8	1911	360	179	0.50	–	–
D9	1990	379	143	0.38	–	1.25% SP-PCE1
D10	1916	365	172	0.47	–	0.21% RR, 0.83% SP-PCE1

Table 2
Binder composition of the dry-mix shotcrete recipes under investigation. The mineralogical and chemical composition of the binder materials is provided in Supplementary Table 1.

Mix. No	Spray Cement	CEM I SR0 1	CAC1	CAC2	SA1	GBFS1	FCC2	MK
	wt-% of binder							
D1	80%	–	–	–	–	20%	–	–
D2	80%	–	–	–	–	20%	–	–
D3	–	93%	–	–	–	–	7%	–
D4	–	90%	10%	–	–	–	–	–
D5	–	70%	10%	–	–	15%	5%	–
D6	70%	–	–	10%	–	20%	–	–
D7	70%	–	–	5%	–	15%	5%	5%
D8	75%	–	–	–	–	15%	5%	5%
D9	70%	–	–	–	–	20%	10%	–
D10	50%	–	3%	7%	–	30%	5%	5%

accelerator was added.

For every mix, fresh concrete was prepared by mixing 1827 ± 74 kg m^{-3} of aggregates (grain size 0–8 mm, see Supplementary Fig. 1), 412 ± 18 kg m^{-3} of binder (cement + SCMs) and water resulting in a water/binder (w/b) ratio of 0.49 ± 0.04. Carbonate aggregates were used for all mixes with the exception of W12, where siliceous aggregates were used in the 0 – 4 mm grain size fraction. Polycarboxylate-based superplasticisers (SP-PCE2 - 5) and in some cases air entrainers (AE1 - 3) or, in the case of W13, a retarder (RE) were added during the mixing process. The detailed mix designs and binder compositions are given in Table 3 and Table 4, respectively.

The cements used were, according to EN 197–1:2018, a CEM I 52.5 R (Type III portland cement according to ASTM C 150), a CEM I 52.5 N SR0, a CEM I 42.5 R SR0 and a CEM II/B-M(S,L,Q) 52.5 N (see Table 4 for details on the composition of the latter). These cements are from now on called CEM I, CEM I SR0 1, CEM I SR0 2 and CEM II, respectively. The additions (SCMs) used were two types of GBFS (GBFS1 and GBFS2), two types of fine limestone (coarser FCC1 and finer FCC2), metakaolin (MK), two types of silica fume (SF1 and SF2) and C-SCM (a commercial combination of different SCMs like GBFS, fly ash and FCC, as specified in the Austrian OENORM B 3309–1, called AHWZ therein) [37].

The fresh concrete, together with the setting accelerator (SA2 - 4), was sprayed into spray panels at a nozzle distance of about 2 m with a flow rate of between 12 and 20 m^3 h^{-1}, using pressurised air with an air flow of approximately 100 m^3 min^{-1}. After a curing time of one day, drill cores with a diameter of 100 mm were taken from the panels (avoiding the panel walls by at least several cm) and stored under tap water for 90 days.

2.2. Lab-scale paste sample fabrication and mix design

Lab-scale preparation of paste samples was performed by either spraying with a MiniShot device or manual mixing and placing to investigate the influence of different accelerator dosages and placing methods on the microstructure of hardened pastes. Details on the paste mix design are given in Supplementary Table 3 and Supplementary Table 4. The samples were prepared from CEM I or CEM I SR0 1 (see chapter 2.1.2), tap water and accelerator SA2 at a w/b of 0.5 and systematically varied accelerator dosages (0, 2, 4, 6, 8 and 10 wt-% relative to the binder mass). 9 paste samples were sprayed with a MiniShot spray test device into PE beakers. Details on the MiniShot device are given in [19,38,39]. The spraying of the full range of accelerator dosages (0–10%) was not possible for CEM I pastes because mixes with high accelerator dosage were too stiff for the spraying process, hence only a maximum dosage of 4% could be sprayed. 12 hand-mixed samples were prepard by manual intermixing of cement and water for 90 s with a portable electric screwdriver (Makita DHP453) with a mounted beater at 1300 rpm. After 10 min the samples were first mixed for 15 s and then again for 30 s while the accelerator was added. The accelerated paste was then immediately transferred into a PE beaker which was vibrated for several seconds with a Vortex mixer (Velp Scientifica ZX4) at 3000 rpm.

In either case, the closed PE beakers containing 5–10 g of sprayed or hand-mixed paste were put into a 20 °C water bath for at least 7 days to ensure isothermal hydration conditions.

2.3. Solid-phase characterization

Mercury intrusion porosimetry (MIP) was performed on all shotcrete mixes and paste samples. For each mixture (see Table 1, Table 3, Supplementary Table 3 and Supplementary Table 4) pieces with a volume of approximately 100–200 mm^3 were used. In the case of hand-mixed and sprayed pastes, they were obtained from the innermost parts of the PE beakers after 28 days. In the case of real-scale shotcrete, the samples were obtained after 90 days from smaller drill cores (22 mm diameter) that had first been drilled from the inner part of the larger water-stored cores, and care was taken to avoid any surfaces that were in contact with the drill and to avoid coarse aggregate particles to minimize their influence on the total pore volume. A solvent exchange method, followed by a low pressure storage, was used to stop hydration and dry the samples, as other drying techniques have been recently rejected as being

Table 3
Mix designs of the wet-mix shotcrete recipes.

Mix. No	Aggregates	Binder	Water	w/b	SA	Admixtures
	kg m^{-3}			-	wt-% rel. to binder	
W1	1889	406	194	0.48	8.0% SA2	1.00% SP-PCE2
W2	1857	411	185	0.45	7.9% SA2	1.00% SP-PCE2
W3	1901	402	184	0.46	7.3% SA2	1.00% SP-PCE2
W4	1852	411	194	0.47	8.2% SA2	1.00% SP-PCE2
W5	1847	409	189	0.46	6.9% SA2	1.00% SP-PCE2
W6	1894	403	182	0.45	10.6% SA2	1.00% SP-PCE2
W7	1811	397	201	0.51	8.1% SA2	1.00% SP-PCE2
W8	1886	401	188	0.47	7.0–8.0% SA2*	1.00% SP-PCE2
W9	1819	400	199	0.50	7.0% SA2	0.60% SP-PCE3
W10	1801	395	208	0.53	7.0% SA2	0.60% SP-PCE3
W11	1754	430	212	0.49	7.0% SA2	0.55% SP-PCE3 + 0.40% AE1
W12	1710 **	411	200	0.49	7.0% SA2	0.75% SP-PCE3
W13	1793	417	208	0.50	7.0% SA2	1.30% SP-PCE4 + 0.40% RE + 0.15% AE2
W14	1830	418	191	0.46	6.0% SA4	1.02% SP-PCE5 + 0.29% AE3
W15	1830	418	191	0.46	9.0% SA3	1.02% SP-PCE5 + 0.29% AE3
W16	1830	418	191	0.46	11.0% SA4	1.02% SP-PCE5 + 0.29% AE3
W17	1830	418	191	0.46	0% ***	1.02% SP-PCE5 + 0.29% AE3
W18	1810	420	198	0.47	9.0% SA3	0.98% SP-PCE5 + 0.21% AE3

*due to low sprayability of W8, the SA dosage could not be measured but only estimated.
** silicate aggregates were used for the 0 – 4 mm grain size fraction.
*** this mix was not sprayed but cast, hence no setting accelerator was added.

too aggressive [9,40]: The pieces were immersed in isopropyl alcohol (IPA) for up to 7 days (solvent/solid volume ratio > 20) to remove the pore water by solvent exchange and then stored in a low pressure cabinet (300 mbar, 25 °C) for several days to remove IPA and subsequently stored under N_2 at room temperature. The MIP measurements of the shotcrete and paste samples were performed on Thermo Scientific Pascal 140 and Pascal 240/440 porosimeters. For W1-W8, 2 to 3 replicate measurements per mix were carried out to determine the uncertainty of the results - in the case of three single measurements, an estimated standard deviation (ESD) was calculated for all derived values. The results obtained from both porosimeters were combined using the SOL.I.D software package and processed assuming cylindrical and plate-like pore shape, a mercury surface tension of 0.48 N m^{-1} and density of 13.5485 g cm^{-3}, and a contact angle of 140° [9,41].

2.4. MIP data processing

The data (given as pore diameter and cumulative pore volume in mm^3 g^{-1}) was processed using deconvolution analysis in the pore diameter range of approximately 100 µm to 7.4 nm (according to an intrusion pressure of 0 to 200 MPa) by using a multi-peaks distribution function fitting to the logarithmic pore size distribution, employing a least-squares parameter optimisation approach. The distribution function was derived from a multi-peak Boltzmann equation (decomposing peaks that overlap with each other), herein called triple Boltzmann equation (TBE), or, where necessary, quadruple Boltzmann equation (QBE) with the general form.

$$\text{TBE}: f(x) = y_0 + A\left(\frac{P_1}{1+e^{\frac{\log\frac{x}{x_1}}{k_1}}} + \frac{P_2}{1+e^{\frac{\log\frac{x}{x_2}}{k_2}}} + \frac{P_3}{1+e^{\frac{\log\frac{x}{x_3}}{k_3}}}\right) \text{ with } P_3 = 1 - P_1 - P_2 \quad (1)$$

Table 4
Binder composition of the wet-mix shotcrete recipes. The mineralogical and chemical composition of the binder materials is given in Supplementary Table 1.

Mix. No	CEM I	CEM I SR0 1	CEM I SR0 2	GBFS1	GBFS2	C-SCM	FCC1	FCC2	SF	SF2	MK
	wt-% of binder										
W1	-	100%	-	-	-	-	-	-	-	-	-
W2	67%	–	–	–	–	33%	–	–	–	–	–
W3	–	90%	–	–	–	–	–	10%	–	–	–
W4	95%	–	–	–	–	–	–	5%	–	–	–
W5	55%	–	–	16%	–	–	10%	13%	7%	–	–
W6	–	60%	–	18%	–	–	–	15%	7%	–	–
W7	55%	–	–	16%	–	–	10%	13%	–	–	7%
W8	–	70%	–	20%	–	–	–	10%	–	–	–
W9 *	66%	–	–	19%	–	–	–	7%	–	–	8%
W10 *	66%	–	–	19%	–	–	–	7%	–	–	8%
W11 *	66%	–	–	19%	–	–	–	7%	–	–	8%
W12 *	66%	–	–	19%	–	–	–	7%	–	–	8%
W13	–	–	100%	–	–	–	–	–	–	–	–
W14	–	68%	–	–	18%	–	–	7%	–	7%	–
W15	–	68%	–	–	18%	–	–	7%	–	7%	–
W16	–	68%	–	–	18%	–	–	7%	–	7%	–
W17	–	68%	–	–	18%	–	–	7%	–	7%	–
W18	–	68%	–	–	18%	–	–	7%	–	–	7%

* For these mixes, the cement and additions as given were mixed together beforehand, yielding a CEM II/B-M(S,L,Q) 52.5 N (CEM II). See text for further explanations.

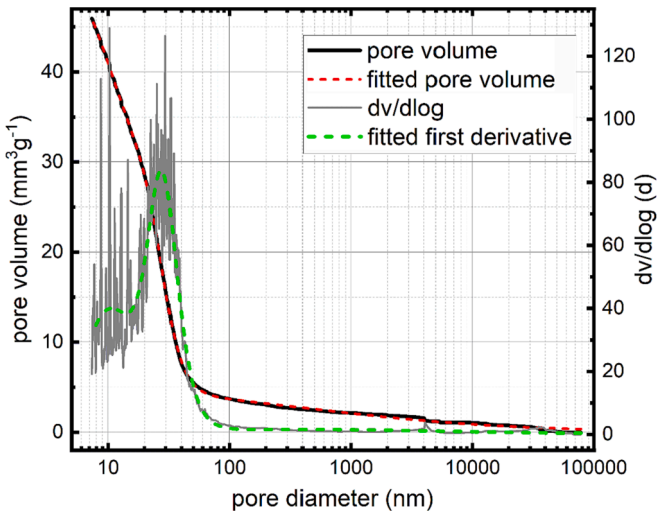

Fig. 3. Example for a pore size distribution curve (in black) fitted with a TBE (in red). The fitted pore volume was used to calculate the d_{25}, d_{50} (median) and d_{75} diameters of the pore size distribution. Note that the value for the critical pore diameter (CPD) can be much more accurately determined from the first derivative of the fitted function (in green) than directly from the derivative of the measured data (in grey).

$$\text{QBE}: f(x) = y_0 + A\left(\frac{P_1}{1+e^{\frac{\log\frac{x}{x_1}}{k_1}}} + \frac{P_2}{1+e^{\frac{\log\frac{x}{x_2}}{k_2}}} + \frac{P_3}{1+e^{\frac{\log\frac{x}{x_3}}{k_3}}} + \frac{P_4}{1+e^{\frac{\log\frac{x}{x_4}}{k_4}}}\right) \text{ with } P_3 = 1 - P_1 - P_2 - P_4 \quad (2)$$

here, $f(x)$ is the intruded volume at a certain pore size (pore diameter or radius) x. y_0 represents a constant factor (*e.g.* the starting intruded volume at the maximum pore size), A is a scale factor (*i.e.* linear term, correlated with P_i), P_1 to P_4 serve as weighting factors for the contribution of the individual terms, and x_1 to x_4 and k_1 to k_4 determine the position and shape of the individual peak distributions. The resulting equations (or, respectively, the first derivative, see Supplementary Equation 1 and Supplementary Equation 2) were used to determine the d_{50} (median), d_{25} and d_{75} values (quartiles, *i.e.* 25 or 75% of the pores are smaller than the d_{25} or d_{75} value, respectively), and the critical pore diameter of the distribution (see also Fig. 3). The pore volume was calculated from the total intruded volume and the mass and bulk density of the sample. The average pore diameter was calculated by the ratio of the pore volume and pore surface in the given pressure range. An example for processing MIP data is attached in the supplement section, demonstrating TBE and/or QBE least-squares parameter optimisation using a spreadsheet program and a numerical solver add-in to determine the critical and median pore diameters and the d_{25} and d_{75} values.

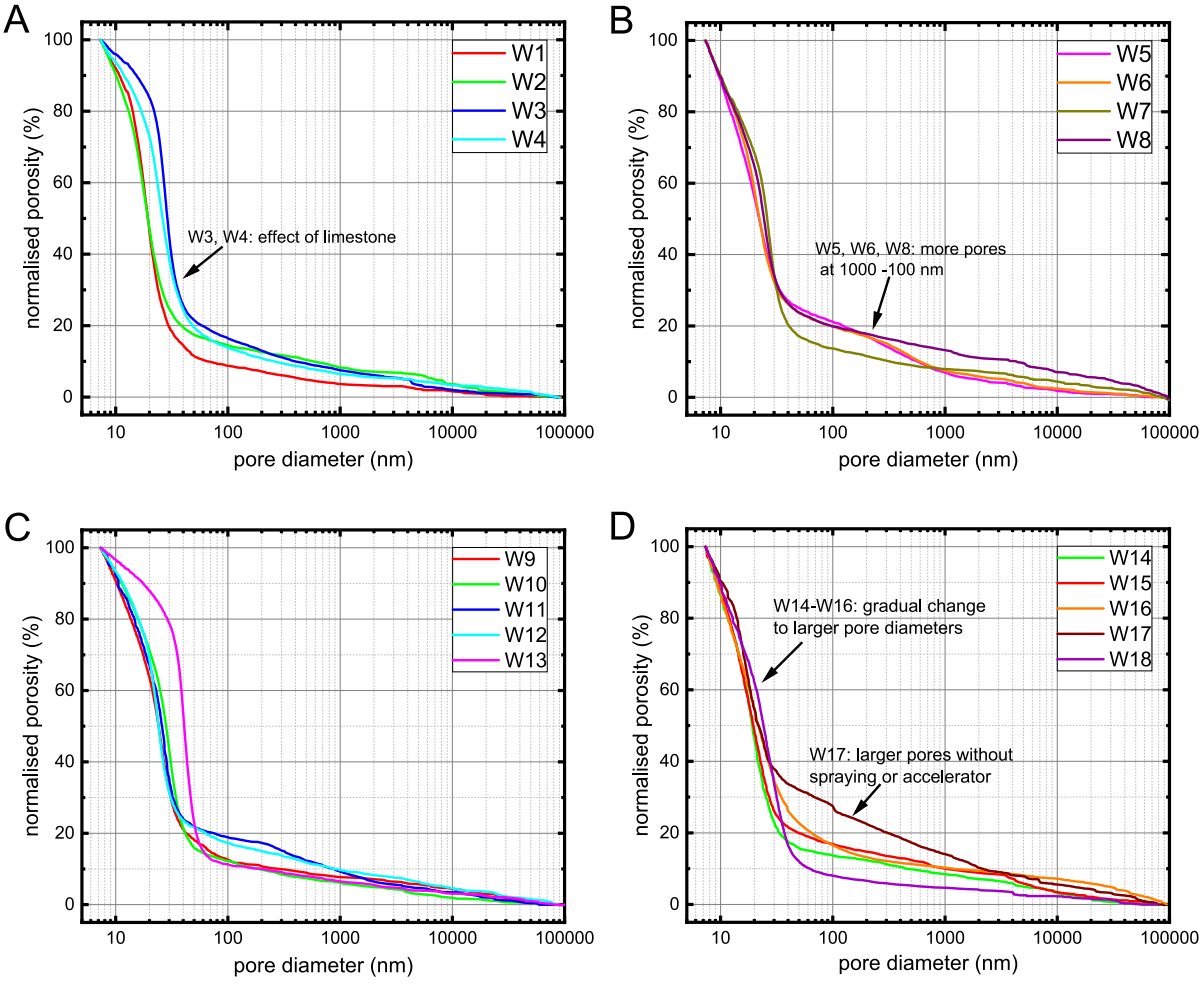

Fig. 4. Pore size distributions of wet-mix shotcretes produced from the following mixes, A: W1-W4, B: W5-W8, C: W9-W13, D: W14-W18. Note the relatively high number of pores in the 1000–100 nm range for W5, W6, W8, W11, W12, the markedly different distribution at 10–50 nm in W13, the high number of large pores in W17 (cast instead of sprayed) and the change in the distribution curve with varying accelerator dosage (W14-W16).

Table 5
Relevant pore size distribution parameters for wet shotcretes, as determined from MIP measurements. For mixes W1-W8, the parameters were averaged from results from two or three measurements per mix. In the case of mixes for which three measurements were performed, an estimated standard deviation (ESD) was calculated (values in brackets).

Mix No.	average DM (nm)	d_{25} (nm)	d_{50} (nm)	d_{75} (nm)	CPD (nm)	Pore volume (%)	Binder
W1	18.8	15.1	19.4	26.4	18.9	8.4	CEM I SR0 1
W2	19.0	14.3	19.4	29.9	18.5	8.5	CEM I + C-SCM
W3	27.7(0.5)	23.8 (1.2)	28.8 (1.2)	42.7 (4.3)	27.8 (1.6)	7.8(1.4)	CEM I SR0 1 + FCC2
W4	23.9(3.1)	19.8 (3.3)	26.5 (4.4)	37.8 (6.1)	26.3 (4.1)	6.8(1.0)	CEM I + FCC2
W5	20.4	13.8	22.0	50.5	21.9	7.7	CEM I + GBFS1 + FCC1 + FCC2 + SF1
W6	20.9	15.0	22.2	47.3	21.5	8.0	CEM I SR0 1 + GBFS1 + FCC2 + SF1
W7	21.6(0.3)	16.8 (1.2)	26.1 (1.3)	35.4 (3.4)	27.2 (1.5)	7.7(1.9)	CEM I + GBFS1 + FCC1 + FCC2 + MK
W8	21.7	15.7	24.3	45.2	24.5	6.6	CEM I SR0 1 + GBFS1 + FCC2
W9	20.9	15.5	24.1	34.7	25.1	6.8	CEM I + GBFS1 + FCC2 + MK
W10	23.2	18.1	28.1	37.0	30.0	11.0	CEM I + GBFS1 + FCC2 + MK
W11	22.7	16.4	25.8	38.1	26.9	8.0	CEM I + GBFS1 + FCC2 + MK
W12	22.9	18.1	24.1	37.0	23.6	9.0	CEM I + GBFS1 + FCC2 + MK
W13	33.4	33.1	40.9	48.7	41.5	8.8	CEM I SR0 2
W14	17.9	13.1	19.2	28.2	19.5	10.7	CEM I SR0 1 + GBFS2 + FCC2 + SF1
W15	18.6	13.1	19.6	31.9	19.7	9.7	CEM I SR0 1 + GBFS2 + FCC2 + SF1
W16	19.5	13.0	21.7	43.6	20.8	13.1	CEM I SR0 1 + GBFS2 + FCC2 + SF1
W17	22.2	14.9	21.5	134.6	17.5	13.3	CEM I SR0 1 + GBFS2 + FCC2 + SF1
W18	19.8	14.6	24.2	33.9	27.4	11.3	CEM I SR0 1 + GBFS2 + FCC2 + MK

3. Results

3.1. Real-scale wet-mix shotcrete

The pore volumes of all wet-mix shotcrete samples lie between 6.6 and 13.3 vol%. Based on triple measurements of W3, W4 and W7, an estimated standard deviation was calculated to be about 1–2 vol% for the pore volume (up to 25% relative error) - this uncertainty in the measured porosities is likely introduced by slightly different amounts of aggregate grains in the sample pieces. Because of this uncertainty in the pore volume, the pore size distributions reported in Fig. 4 (for each set of wet-mix shotcretes, *i.e.* W1-W8, W9-W13 and W14-W18) are normalised for better comparability. The average pore diameters lie between 17.9 and 33.4 nm, median pore diameters (d_{50}) between 19.2 and 40.9 nm and critical pore diameters (CPD) between 17.5 and 41.5 nm (see Table 5).

Shotcretes produced with either pure CEM I SR0 1 or CEM I substituted by 33 wt-% of C-SCM (*i.e.* W1 and W2) exhibited relatively fine pore distribution curves with average pore diameters of 18.9 ± 0.1 nm, CPDs of 18.7 ± 0.2 nm and median pore diameters of 19.4 ± 0.1 nm. The substitution of CEM I or CEM I SR0 1 by 5–10 wt-% of fine limestone without any other additions (*i.e.* W3 and W4) causes a shift in the pore size distribution towards larger pore diameters: these samples exhibit average pore diameters of 25.8 ± 1.9 nm, CPDs of 27 ± 0.8 nm and median pore diameters of 27.7 ± 1.1 nm. Combined SCM additions with GBFS, FCC and SF (W5, W6, W14-W17) resulted in pore size distributions similar to W1 and W2, with average pore diameters of 20.0 ± 2.1 nm, CPDs of 19.7 ± 2.2 nm and median pore diameters of 20.7 ± 1.5 nm. In contrast, mixes with combined SCM additions without SF, but with GBFS, FCC and with or without MK (W7, W8, W9-W12, W18) displayed similar average pore diameters of 21.5 ± 1.7 nm, but higher median pore diameters and critical pore diameters of 26.1 ± 2.0 nm and 26.8 ± 3.2 nm, respectively. The shotcrete mix produced with CEM I SR0 2 and high amounts of superplasticiser (W13) had the largest pore size distribution of all investigated wet-mix shotcretes, with an average pore diameter of 33.4 nm, median pore diameter of 40.9 nm and critical pore diameter of 41.5 nm.

Comparing W14-W17 (same mix design and binder composition, but varying accelerator dosage), non-sprayed non-accelerated concrete (*i.e.* W17) exhibited more pores in the range of 50–1000 nm, resulting in higher average pore diameters. The shotcrete mixes W14-W16 show average, median and critical pore diameters that increase with the

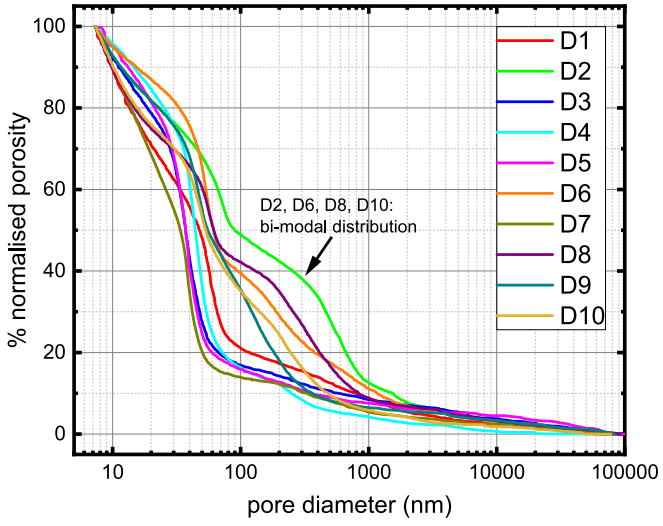

Fig. 5. Pore size distributions of dry-mix shotcretes. Note the higher number of large pores (>100 nm) in samples from the mixes D2, D6, D8, D9 and D10 in comparison to the other dry-mix shotcretes.

Table 6
Relevant pore size distribution parameters for dry-mix shotcrete, as determined from MIP measurements.

Mix No.	average DM (nm)	d_{25} (nm)	d_{50} (nm)	d_{75} (nm)	CPD (nm)	Pore volume (%)	Binder
D1	26.2	16.6	48.0	75.7	56.5	9.7	SpC + GBFS1
D2	39.9	32.8	92.3	554.1	65.4	8.2	SpC + GBFS1
D3	27.8	24.0	37.1	53.3	36.4	8.6	CEM I SR0 1 + FCC2
D4	33.3	31.4	44.3	59.1	44.9	8.5	CEM I SR0 1 + CAC1
D5	29.5	25.7	37.0	49.8	37.8	7.0	CEM I SR0 1 + CAC1 + GBFS1 + FCC2
D6	42.8	41.6	61.3	253.2	53.2	7.7	SpC + CAC2 + GBFS1
D7	23.3	16.3	33.8	44.7	39.4	9.6	SpC + CAC2 + GBFS1 + FCC2 + MK
D8	31.4	19.8	61.8	328.7	55.6	8.2	SpC + GBFS1 + FCC2 + MK
D9	34.8	31.5	55.8	147.2	45.8	8.6	SpC + GBFS1 + FCC2
D10	30.5	21.2	53.8	188.2	48.7	8.4	SpC + CAC1 + CAC2 + GBFS1 + FCC2 + MK

accelerator dosage (6–11 wt-% relative to the binder).

3.2. Real-scale dry-mix shotcrete

The pore size distribution curves for the dry-mix shotcretes are reported in Fig. 5. The measured pore volumes lie in a range similar to wet-mix shotcrete, with values between 7.0 and 9.7 vol%. The pore distribution is shifted to larger diameters in comparison to wet-mix shotcretes, with average pore diameters between 23.3 and 41.6 nm, median pore diameters between 33.8 and 92.3 nm and CPDs between 36.4 and 65.4 nm (see Table 6). Several mixes (D2, D6, D8, D9 and D10, all with spray cement, w/b $\leq$ 0.50 and $\geq$ 20% of GBFS + MK) exhibit a large number of pores in the range of 100–1000 nm. In D2, D6, D8 and D10 this is also associated with a distinctly bimodal pore size distribution curves (*i.e.* two particularly steep increases instead of one increase typical for MIP distribution curves of cementitious systems). The modes (*i.e.* the critical pore diameters) for this first increase lie between 198 nm for D6 and 547.4 nm for D2. Dry-mix shotcretes sprayed with CEM I SR0 1 and setting accelerator or CAC (*i.e.* D3-D5) have very similar pore size distribution, which is also not significantly different to some mixes sprayed with spray cement (D1, D7).

3.3. Hand-mixed paste samples

The pore size distribution curves for the hand-mixed paste samples prepared with either CEM I or CEM I SR0 1 at increasing accelerator dosages are reported in Fig. 6. The pore volumes and pore size distributions are varying as a function of accelerator addition: i) the average, median and critical pore diameter of all samples are steadily increasing with increasing accelerator addition (Table 7); ii) the pore volume is significantly decreasing for samples with CEM I SR0 1 from 24.5 to 22.0 vol%; iii) for CEM I samples the addition of 2% accelerator causes a decrease in the pore volume from from 20.9 to 19.1 vol%, but further accelerator addition results in increasing pore volume close to 22 vol%. On average, the pore volume and pore size distribution values are lower for CEM I pastes than for CEM I SR0 1 pastes.

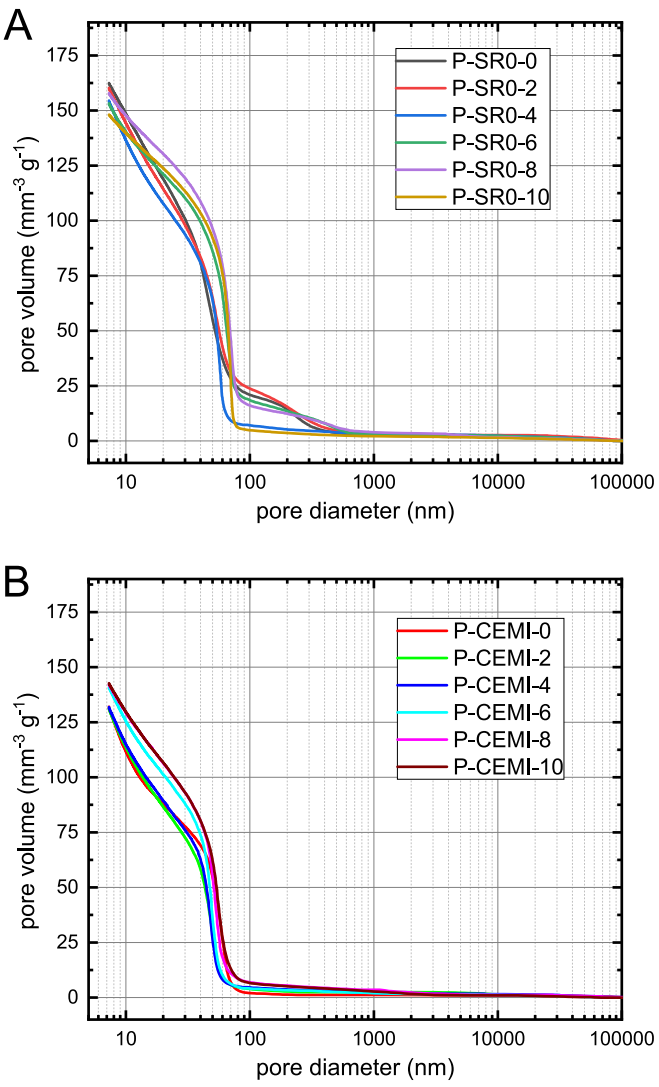

Fig. 6. Pore size distributions of hand-mixed accelerated paste mixes prepared with CEM I SR0 1 (A) and CEM I (B) at systematically increasing accelerator dosages.

3.4. Sprayed paste samples

The pore size distribution curves for paste samples that were sprayed with the MiniShot device are reported in Fig. 7 and derived values are given in Table 8. For pastes prepared with CEM I SR0 1, the average, median and critical pore diameter and the pore volume steadily increase with increasing setting accelerator dosage. For pastes containing CEM I, all values are decreasing from 0 to 2 wt-% accelerator dosage but then increase at a dosage of 4 wt-% - spraying at dosages > 4 wt-% was not possible (see also chapter 2.2). This initial decrease at low accelerator dosages was also observed for hand-mixed CEM I pastes.

The pore volume, the average, median and critical pore diameter of all sprayed paste samples lie within 23.8 $\pm$ 3.6 vol%, 37.1 $\pm$ 11.3 nm, 62.3 $\pm$ 20.2 nm and 70.6 $\pm$ 19.4 nm, respectively (Table 8), which are values markedly higher than those reported for the real-scale wet-mix shotcrete (Table 5) or for hand-mixed pastes (Table 7). However, when

Table 7
Relevant pore size distribution parameters for hand-mixed pastes, as determined from MIP measurements.

Sample	average DM (nm)	d_{25} (nm)	d_{50} (nm)	d_{75} (nm)	CPD (nm)	Pore volume (%)	Binder
P-SR0-0	25.8	18.6	39.8	57.5	47.0	24.5%	CEM I SR0 1 + 0% SA2 – hand-mixed
P-SR0-2	25.4	17.2	42.0	61.7	54.2	24.8%	CEM I SR0 1 + 2% SA2 – hand-mixed
P-SR0-4	23.6	15.8	41.9	56.1	56.1	24.3%	CEM I SR0 1 + 4% SA2 – hand-mixed
P-SR0-6	30.1	25.6	55.9	68.2	64.7	23.6%	CEM I SR0 1 + 6% SA2 – hand-mixed
P-SR0-8	33.2	31.2	60.7	71.3	68.5	22.0%	CEM I SR0 1 + 8% SA2 – hand-mixed
P-SR0-10	33.4	32.5	61.4	68.5	68.0	22.0%	CEM I SR0 1 + 10% SA2 – hand-mixed
P-CEMI-0	21.9	13.4	43.1	58.0	60.4	20.9%	CEM I + 0% SA2 – hand-mixed
P-CEMI-2	21.4	14.2	35.1	48.7	48.4	19.1%	CEM I + 2% SA2 – hand-mixed
P-CEMI-4	22.1	14.9	38.1	48.5	47.8	20.7%	CEM I + 4% SA2 – hand-mixed
P-CEMI-6	23.8	17.2	41.8	50.2	49.2	21.7%	CEM I + 6% SA2 – hand-mixed
P-CEMI-8	26.0	19.8	45.3	54.2	52.4	21.8%	CEM I + 8% SA2 – hand-mixed
P-CEMI-10	26.1	19.6	45.8	57.5	55.8	21.6%	CEM I + 10% SA2 – hand-mixed

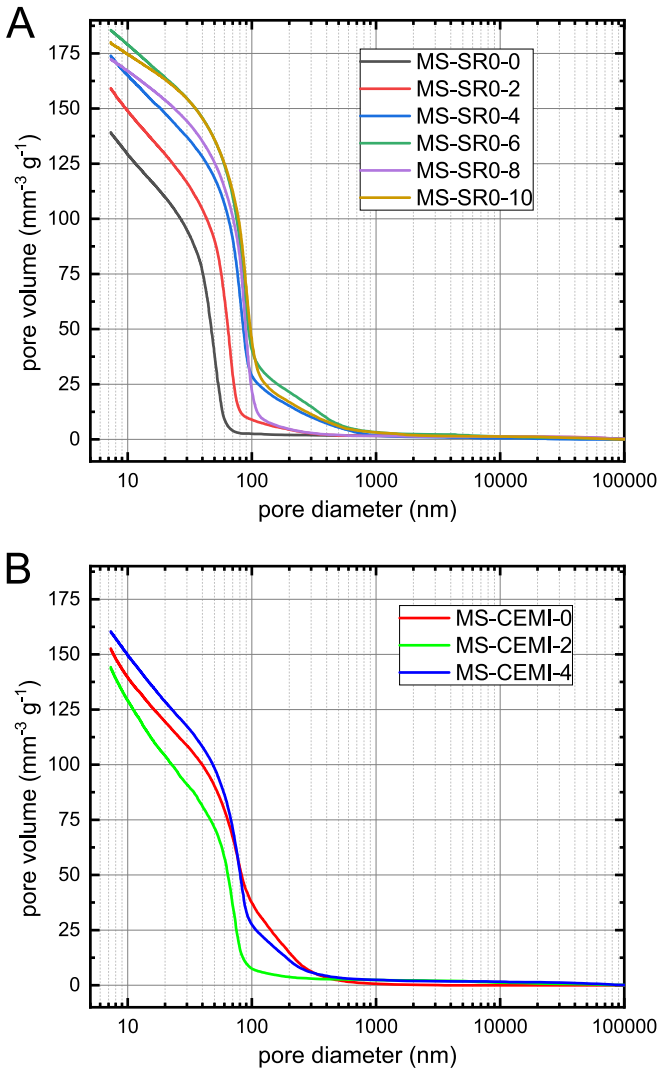

Fig. 7. Pore size distributions of sprayed accelerated paste mixes with CEM I SR0 1 (A) and CEM I (B). Note the change in the distribution curve with increasing accelerator dosage (0–10 wt-% and 0–4 wt-% by binder).

compared regarding the influence of the accelerator, the same trends can be observed for hand-mixed and sprayed pastes: in both cases pore size distribution values are increasing with increasing accelerator dosage, with the exception of pore volume in the case of CEM I SR0 1, which is decreasing for hand-mixed but increasing for sprayed paste samples.

4. Discussion

In this study, we analyse and compare the porosity and pore size distribution of a large set of accelerated shotcrete samples prepared with the wet- and dry-mix shotcrete process. We also investigate hand-mixed pastes and pastes sprayed with a MiniShot device. Systematic variations in the mix designs allow characterizing the influence of different fabrication techniques, binder compositions, organic admixtures, accelerator dosages and the spraying process itself. The pore size distributions were analysed by least-squares optimisation of multi-peak Boltzmann distribution equations.

The deconvolution analysis allows accurate determination of the critical pore diameter in contrast to directly extracting this value from the distribution curves. The functions enable the approximation of even complex multi-modal pore size distributions with hundreds of datapoints by 9–12 empirically calibrated independent parameters. This approach could also be used to generate pore size distributions with systematic variations, *e.g.* for modelling purposes.

4.1. Remarks on the deconvolution analysis

The pore size distribution curves of all mixes could successfully be fitted to TBEs (Equation 1), using 9 parameters. However, for some real-scale shotcrete mixes which exhibited bimodal pore distribution (*i.e.* the distribution curve increases in two places resulting in a significant "bump", *e.g.* W11 or D2) and for all paste mixes a QBE (Equation 2) was used for the data fitting (using 12 parameters), resulting in a much lower sum of squared residuals compared to TBE. To give an additional indication for the quality of the fitted equations, an R^2 value was calculated for all mixes according to Supplementary Equation 3 (see supplementary section). The results (see Supplementary Table 5) show that very good fits were achieved for all mixes, even those with bimodal distributions, with 9–12 independent parameters. To the best of the author's knowledge, there is no description of such deconvolution analysis of pore size distributions, demonstrated here using a set of 50 cementitious samples. We therefore suggest that these equations can be used for more accurate parameter determination and novel modelling approaches to investigate the microstructure-property-relationships of concrete and its changes with mix design and during hydration. For example, a limited (most characteristic) set of parameters could be used to derive the dependence of *e.g.* transport properties on material features such as pore size distribution or permeability [42,43].

4.2. Influences on the porosity of shotcrete and accelerated pastes

The pore size distribution values and pore volumes of the shotcrete samples are similar to previously reported data obtained from MIP

Table 8
Relevant pore size distribution parameters for sprayed pastes, as determined from MIP measurements.

Sample	average DM (nm)	d25 (nm)	d50 (nm)	d75 (nm)	CPD (nm)	Pore volume (%)	Binder
MS-SR0-0	26.9	23.7	42.1	50.9	51.1	23.2%	CEM I SR0 1 + 0% SA 2 – MiniShot
MS-SR0-2	31.1	27.6	55.0	67.0	67.1	25.3%	CEM I SR0 1 + 2% SA 2 – MiniShot
MS-SR0-4	38.3	37.6	72.1	88.0	80.7	25.5%	CEM I SR0 1 + 4% SA 2 – MiniShot
MS-SR0-6	44.6	47.1	78.5	96.0	85.3	25.5%	CEM I SR0 1 + 6% SA 2 – MiniShot
MS-SR0-8	44.0	46.5	78.4	91.2	87.9	26.4%	CEM I SR0 1 + 8% SA 2 – MiniShot
MS-SR0-10	48.4	50.9	82.6	99.8	90.0	27.4%	CEM I SR0 1 + 10% SA 2 – MiniShot
MS-CEMI-0	31.4	24.2	62.9	98.1	75.6	22.9%	CEM I + 0% SA 2 – MiniShot
MS-CEM-2	25.7	17.3	49.0	70.1	69.5	20.2%	CEM I + 2% SA 2 – MiniShot
MS-CEMI-4	33.1	26.8	64.5	85.6	78.6	24.6%	CEM I + 4% SA 2 – MiniShot

measurements [25,27,29]. Lagerblad et al. [28] also reported data for hand-mixed accelerated pastes that exhibit CPDs similar (about 50–70 nm) to the results presented in this study. Interestingly, the pore volumes for wet-mix shotcrete presented in this study are similar to values which have been obtained from water accessible porosity tests on wet-mix shotcrete [24], however for dry-mix shotcrete higher values (15–19 vol-%) have been reported with this method [18]. It is possible that dry-mix shotcretes exhibit significantly more pores > 100 µm, which are inaccessible to MIP but could be measured by water accessible porosity and thus result in higher porosities measured with the latter method.

We want to stress that, despite the other influences discussed in the following chapters, measurement errors along the analysis chain (sampling, drying, MIP measurement, also aggregate distribution where applicable) can introduce uncertainties and data scatter: Based on replicate measurements of three real-scale wet-mix shotcrete samples (see Table 5), standard deviations were estimated for the derived parameters: up to 3.1 nm (13.0% relative error) for the average, up to 4.4 nm (16.4% relative error) for the median and up to 4.1 nm (15.7% relative error) for the critical pore diameter. In shotcrete samples inhomogeneous aggregate distribution can also heavily influence the determined pore volume (see chapter 3.1).

4.2.1. *Influence of fabrication technique*

Without doubt, the nature of the spraying process and the spraying technique itself (*i.e.* wet-mix *vs* dry-mix spraying) exert a strong influence on the pore size distribution. This influence can be characterised - amongst others - by the median and critical pore diameter, which are given in a cross-plot of all investigated mixes in Fig. 8. Due to the nature of pore size distributions, both values are usually quite similar - for an ideal (normal) distribution, their ratio would be 1. Indeed, for all wet-mix shotcretes the ratio between critical and median pore diameter is close to this value (represented by a black line in Fig. 8), but the values from other sample series (such as pastes and some dry-mix shotcretes) differ from this ideal ratio.

Mixes that plot to the right of the black line (such as the dry-mix shotcretes D2, D6, and D8-D10) exhibit larger median pore diameters due to a high number of pores larger than the critical pore diameter (*cf.* Fig. 5). Dry-mix shotcretes produced with CEM I SR0 1 (the same cement that was used for wet-mix shotcrete) are, similar to wet-mix shotcrete, plotting close to the 1:1 ratio. These observations made with the aid of Fig. 8 indicate that the dry-mix spraying process causes relatively large pore sizes compared to the wet-mix process, and certain dry mixes have a critical to median pore diameter ratio markedly < 1. This could be caused by (i) lower compaction forces in the dry-mix process due to lower spraying rates (2.5 $m^3 h^{-1}$ *vs* ≥ 12 $m^3 h^{-1}$), (ii) short contact time and subsequently less interaction between water and binder in the dry spraying process, (iii) the lower binder content and (iv) compositional differences between the wet- and dry-mix shotcretes, such as the use of air-entrainers in some wet-mix shotcrete or the use of fast-setting spray cement for dry-mix shotcrete [21] (see Supplementary Table 1).

In contrast, the hand-mixed and sprayed paste samples plot on the left of the black line in Fig. 8, thus exhibiting a notably higher number of pores below the critical pore diameter, causing the median pore diameter to be shifted to smaller values. This together with a comparison of

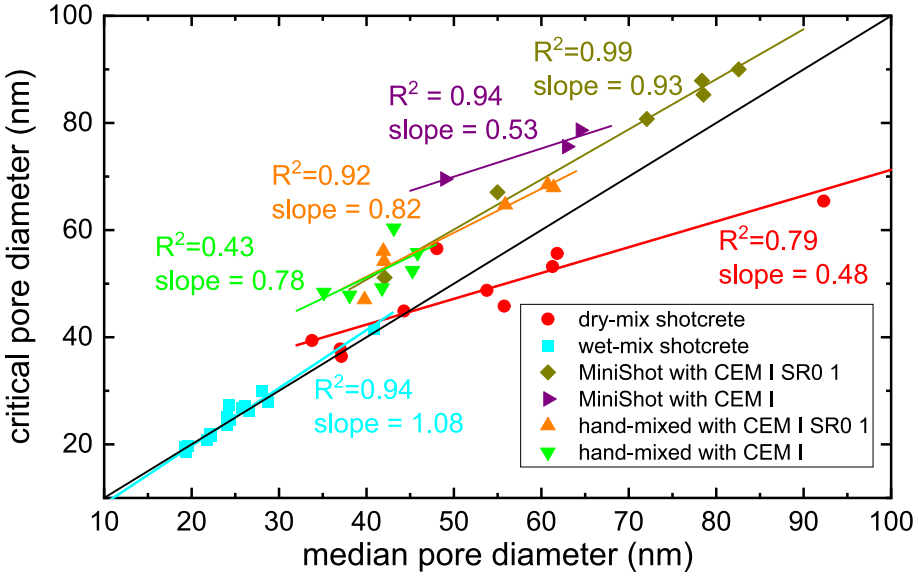

Fig. 8. Cross-plot of median and critical pore diameters of the investigated shotcrete and paste mixes. While all wet-mix shotcretes display a ratio close to one (represented by the black line), for hand-mixed and sprayed pastes and certain dry-mix shotcretes the critical pore diameter significantly differs from the median pore diameter.

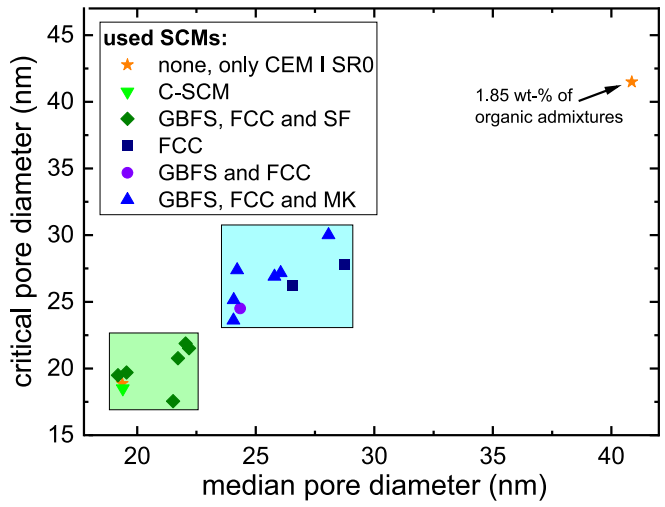

Fig. 9. Possible influences of SCMs and organic admixtures on the pore size distribution of wet-mix shotcrete. All mixes (except one outlier: W13 with a particularly high content of organic admixtures) can be classified into two separate groups with either C-SCM or GBFS + FCC + SF with lower critical and median pore diameters (green rectangle) or FCC and/or GBFS + FCC with MK with higher values (blue rectangle). One sample, containing relatively high amounts of organic admixtures, lies outside of these groups. See text for further explanations.

the pore volumes shows that hand-mixing or spraying accelerated cement pastes can result in coarse (*i.e.* high average, median and critical pore diameters) but relatively narrow pore size distributions and high pore volume, which is likely caused by the absence of aggregates and admixtures and the different or absent spraying process.

4.2.2. *Influence of SCMs and organic admixtures*

Besides the fabrication process, the binder composition and the use of organic admixtures can also influence the pore size distribution (Fig. 9). The latter is evident from the comparison of the wet-mix shotcrete mixes W1 and W13: these mixes have very similar mix designs except for a relatively high amount (1.85 wt-% of binder mass) of organic admixtures (PCE-based superplasticiser, tenside-based air entrainer and retarder, marked by arrow in Fig. 9) contained in W13, which consequently has more than double the median and critical pore diameter of W1. It is possible that such relatively high amounts of organic admixtures can negatively influence ongoing hydration and by extent microstructure refinement, leading to coarser pore size distribution, but there is not sufficient data to support a more precise conclusion. We suggest that further research can elucidate the role of organic admixtures on the porosity of shotcrete.

All other wet-mix shotcretes exhibit arguably very similar pore size distributions when compared to dry-mix shotcrete or normal concrete. Although a certain data scatter is likely introduced by sample preparation and measurement, two likely distinct groups can be identified (marked by rectangles in Fig. 9) based on their different binder compositions: i) mixes with binder compositions of either CEM I or CEM I SR0 1 with only FCC (*i.e.* W3 and W4) exhibited relatively high median and critical pore diameters, similar to mixes with GBFS and FCC (W8) plus MK (W7, W9-W12, W18). ii) mixes with C-SCM or GBFS, FCC and SF (W2, W5, W6, W14-W17) displayed markedly lower median and critical pore diameters. We presume that adding only calcium carbonate like FCC to the binder results in increased packing density but also increased water demand [44,45], leading to a slight increase in the pore sizes of shotcrete due to an increased ratio of water to reactive binder mass – however, it is also possible that FCC partaking in chemical reactions [16] comes into effect. The influence of FCC can apparently be mitigated by combining it with additional SF, but less so with additional GBFS or MK. We suggest that this might be due to possible differences in the particle size, hydration reaction (*e.g.* C(A)SH-formation) and/or accelerator interaction of SF *vs* GBFS and MK.

4.2.3. *Influences of the accelerator addition*

In all hand-mixed and MiniShot-sprayed paste samples and in selected large-scale wet-mix spraying tests, the accelerator dosage was varied systematically from 0 up to 11 wt-% per binder. For MIP results of sprayed and hand-mixed pastes made with either CEM I or CEM I SR0 1, a clear influence of the amount of accelerator used can be observed (Fig. 10A and B): The pore volume and the average, critical and median pore diameters are significantly changing between accelerator dosages of 0–10%: most of the values are steadily increasing with increasing accelerator dosages. Presumably, this behaviour is due to the accelerator addition which may influence pore volume and pore size distribution by: i) the almost instantaneous setting of the paste and the formation of ettringite needles impairing proper compaction and obstructing ongoing cement hydration and pore refinement [28], ii) short and long-term changes in the phase assemblage of the cement matrix [16] and iii) possibly additional water added as part of the accelerator suspension/solution (although recent studies have shown ettringite formation to consume the water added by the accelerator [21]). However, at very low accelerator dosages (up to 2 wt-%), the pore-filling effect of the newly formed ettringite needles may counteract these effects, actually lowering the pore volume and refining the pore size distribution. This effect is presumably visible in the case of CEM I pastes, for which an initial decrease in the pore volume and pore size distribution parameters is observed.

For real-scale shotcrete (Fig. 10C) the relationship between porosity and accelerator is more difficult to assess, as no non-accelerated sprayed concrete was investigated (W17 was not sprayed). For the observed accelerator dosage from 6 to 11 wt-%, the average, median and critical pore diameter are increasing, while the increase in the pore volume is less clear, likely due to the influence of the aggregates (cf. chapter 3.1) and variations in the binder composition. In contrast to data published based on water-accessible porosity (*e.g.* [46]), non-sprayed and non-accelerated concrete (*i.e.* W17) exhibited about the same pore volume (13.3 vol-%) as its sprayed and accelerated counterparts.

We presume that the influence of the accelerator addition causes increased permeability of the cement matrix in the hardended paste or shotcrete. This may be a possible explanation for the often-observed decreased strength and durability of shotcrete in comparison to non-accelerated concrete [12,16,17,24,28,47]. When producing wet-mix shotcrete, the accelerator dosage should be carefully adjusted to fulfill early strength requirements but limit the deleterious effect of the accelerator on late strength and durability and mitigate the environmental impact of shotcrete accelerators [22].

4.2.4. *Influences of the cement and the spraying process*

An exception of the trends observed in the previous chapter 4.2.3 and Fig. 10 can be seen in the pore volume of CEM I SR0 1 pastes: with increasing accelerator addition, the pore volume is decreasing for hand-mixed samples but increasing for MiniShot-sprayed samples. In contrast, CEM I sprayed and hand-mixed pastes show similar trends regarding the pore volume. In general significant differences can be observed between the cements, with the pore volume and average, median and critical pore diameter being usually lower for CEM I than for CEM I SR0 1 at given accelerator dosages. However, without accelerator, CEM I paste samples actually have coarser pore size distributions (Fig. 11). These different behaviours are likely caused by the cements having different physico-chemical composition (*e.g.* different contents of C_3A and calcium-sulfate-based setting regulators) and resulting in different hydration products which influences the development of the pores: In the absence of accelerator, CEM I SR0 1 paste is more workable than CEM I pastes and therefore compaction and spraying quality is improved, with the spraying processes delivering lower pore volumes than hand-mixing.

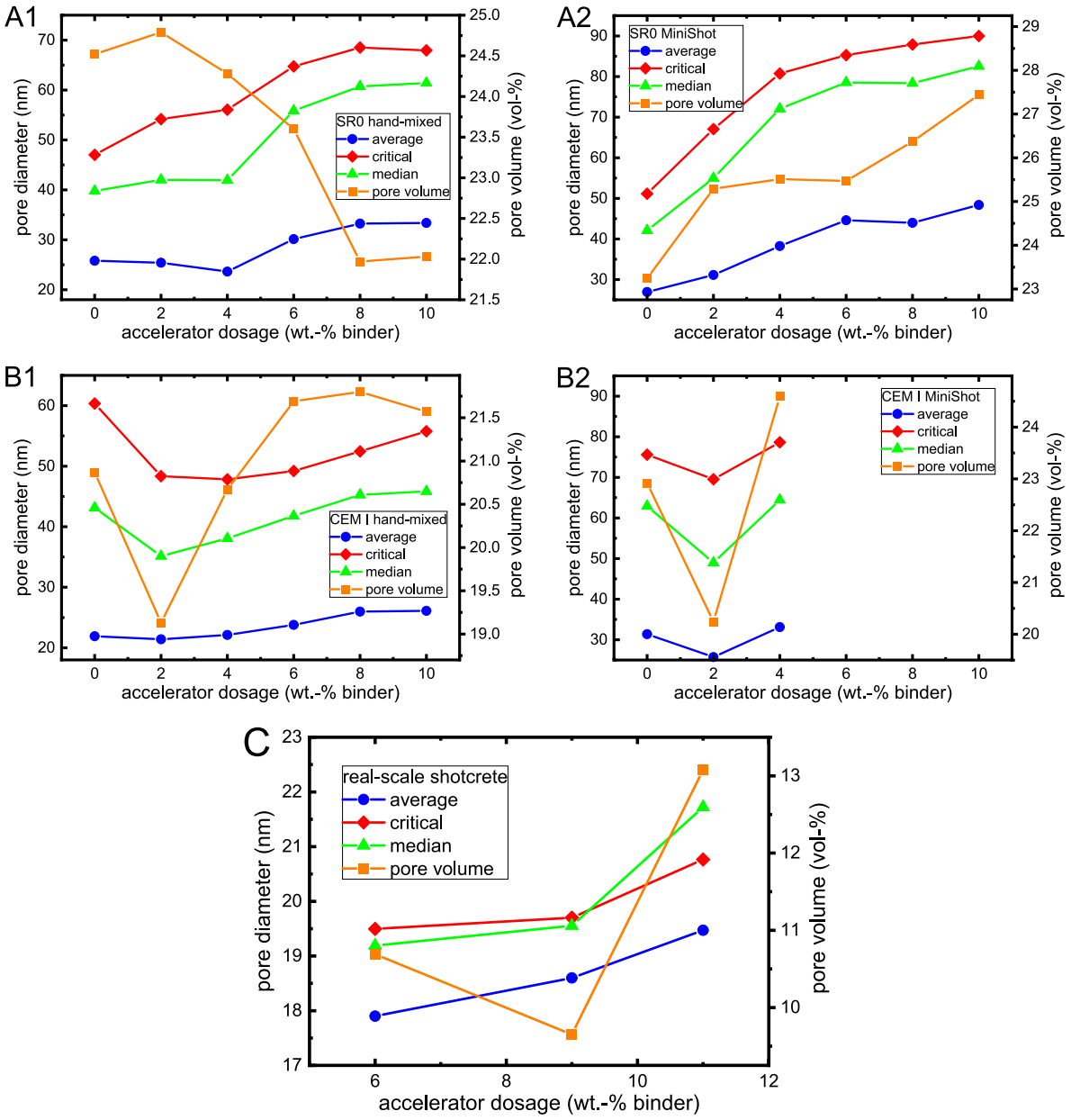

Fig. 10. Influence of the accelerator dosage on the pore size distribution and pore volume. (A1/2) hand-mixed and MiniShot-sprayed CEM I SR0 1 paste samples, (B1/2) hand-mixed and MiniShot-sprayed CEM I paste samples, (C) real-scale sprayed concrete samples. See text for further explanations.

With the addition of the accelerator, this advantage of CEM I SR0 is gradually diminished and the pore volume and pore size distribution significantly change with increasing accelerator addition. On the other hand, CEM I produces stiffer, less workable pastes even if no accelerator is added, and low accelerator additions of 2 wt-% actually decrease the pore volume and refine the pore size distribution.

Besides the accelerator addition and the cement, the spraying process itself also causes significant differences in the porosity of paste samples. A comparison of all hand-mixed and sprayed paste samples (Fig. 11) reveals that the spraying process usually results in higher pore volume (with the exception of non-accelerated CEM I SR0 1) and coarser pore size distribution than hand–mixing for a given accelerator dosage: The pore volume, average, median and critical pore diameter of sprayed samples are on average 10, 36, 41 and 34% higher than their non-sprayed counterparts. This could be because of i) lower compaction by the MiniShot spray device for the sprayed samples than by the Vortex mixer for lab-mixed samples, ii) different reactivity of the paste due to the spraying [48], iii) differences in the paste preparation between the MiniShot spraying and the hand-mixing process in the lab (*e.g.* mix energy or accelerator distribution [49,50]). These findings corroborate again the long-standing view that lab-mixed accelerated or non-accelerated pastes, mortars or concretes are not perfect analogies for their sprayed counterparts (*e.g.* [35,48]). Due to obvious differences in the microstructure, especially tests where permeability plays an important role, such as tests regarding the uptake of substances (*e.g.* sulfate attack, chloride ingress, carbonation), should be performed on sprayed materials rather than their lab-mixed analogues (paste or concrete).

4.3. Combined discussion

The largest influence on the porosity of shotcrete is arguably excerted by the type of the spraying process. Large differences were determined between dry-mix and wet-mix shotcretes on the one side and

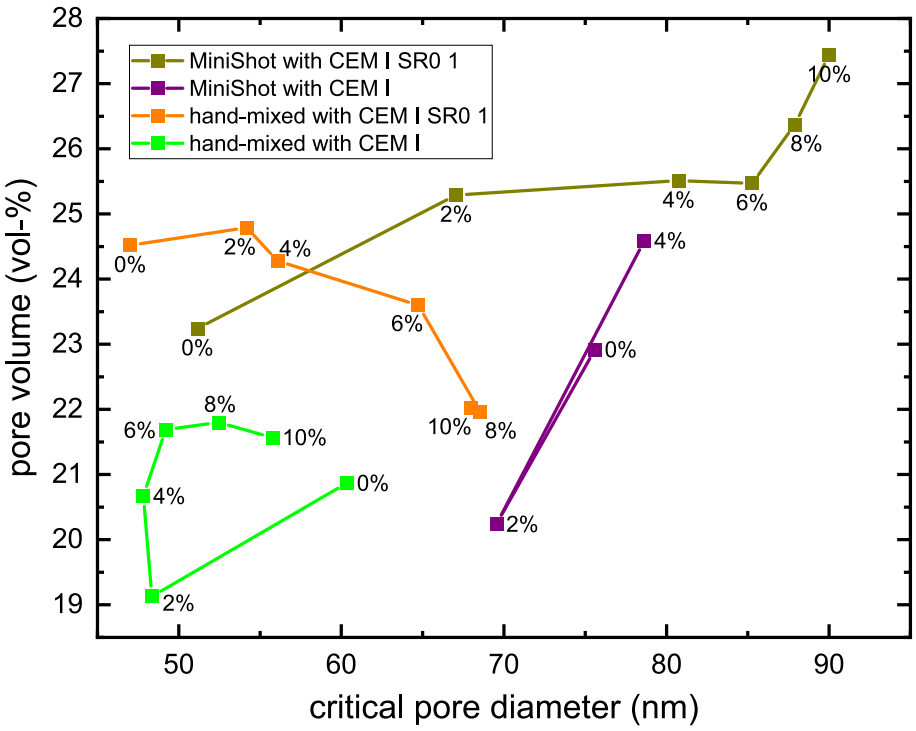

Fig. 11. Comparison of sprayed and hand-mixed cement pastes prepared with either CEM I or CEM I SR0 1. Percentage labels give the used accelerator dosage in wt-% per binder. Notice the large differences between hand-mixed and sprayed pastes and the differences between CEM I and CEM I SR0 1 samples.

between hand-mixed and MiniShot-sprayed pastes on the other. Dry-mix shotcrete, produced with fast-setting spray binders, exhibits overall larger pores (as represented by high average, median and critical pore diameters) than wet-mix shotcrete. Due to the inhomogeneous aggregate distribution, the pore volume of real-scale shotcrete can only be determined with an accuracy of ± 2 vol-%. Furthermore, the spraying process itself caused a significant influence on the porosity, as pastes sprayed with the MiniShot device exhibit different pore volumes and a significantly coarser pore size distribution (*i.e.* higher average, median and critical pore diameters) compared to hand-mixed (*i.e.* non-sprayed) pastes both with and without setting accelerator.

The binder composition was found to influence the porosity of particularly wet-mix shotcrete and pastes: Shotcretes or pastes with either pure C_3A-free CEM I or a combination of additions (either pre-mixed C-SCM or GBFS + FCC + SF) exhibit notably lowered median and critical pore diameters in comparison to samples with pure ordinary CEM I or mixes with FCC and GBFS with or without MK. Accelerated pastes made with CEM I had a smaller pore volume and finer pore size distribution than pastes made with CEM I SR0 1. In addition, the use of high amounts (*e.g.* > 1 wt% of binder mass) of organic admixtures such as superplasticizer might lead to especially large pores.

The addition of a setting accelerator increases the pore volume of the samples as well as the average, median and critical pore diameter in sprayed pastes made with normal CEM I or C_3A-free CEM I SR0 1. For sprayed CEM I SR0 1 pastes the pore volume, average, median and critical pore diameter increase from an accelerator dosage of 0 to 10 wt-% per binder by 18, 80, 96 and 76%, respectively. We recommend limiting the accelerator dosages to the amount required for sufficient early-strength development to prevent unnecessarily high shotcrete permeability and decreases in final strength.

Our findings and new extensive datasets suggest an as-of-yet unused potential of MIP to be used for the assessing of new shotcrete mix designs towards the systematic influence of different additions and admixtures and to characterize the influence that spraying will have on a certain mix design. This approach can help to identify (shotcrete) mix designs with pore size distributions favourable for certain properties - for example reduced permeability to increase durability against the ingress of harmful chemical compounds such as those involved in sulfate or chloride attack or carbonation.

5. Conclusions

Although the influence of key factors such as binder composition and mix design on pore volume and pore size distribution has been analysed in literature many times for “normal” (cast-in-place) concrete, little has been published concerning these connections and additional aspects within the shotcrete research field. The main findings from this study about the porosity of shotcrete and accelerated pastes are summarized as follows:

1. Newly developed multimodal distribution functions allow more accurate determination of the critical pore diameter from MIP measurements. Moreover, pore size deconvolution could help to correlate pore size distributions with materials properties, *e.g.* increased durability, as a promising direction for future research.
2. The type of the spraying process has a large effect on porosity. Dry-mix shotcrete exhibits overall coarser pore size distribution than wet-mix shotcrete. Furthermore, pastes sprayed with a lab-spraying device (MiniShot) exhibit on average higher pore volume and a significantly coarser pore size distribution than hand-mixed pastes.
3. The binder composition of wet-mix shotcrete and paste influences the porosity: Shotcretes or pastes with pure and blended C_3A-free CEM I (pre-mixed C-SCM or GBFS + FCC + SF) exhibit finer pore size distribution than pure and (FCC, GBFS and MK) blended ordinary CEM I.
4. Accelerated pastes made with CEM I had a smaller pore volume and finer pore size distribution than pastes made with CEM I SR0 1. High amounts of organic admixtures such as superplasticizer might lead to especially large pores.
5. The addition of a setting accelerator leads to increased pore volume and coarser pore size distributions in sprayed pastes made with normal CEM I or C_3A-free CEM I SR0 1. We recommend limiting the

accelerator dosages to the amount required for sufficient early-strength development to prevent unnecessarily high shotcrete permeability and decreases in final strength.

CRediT authorship contribution statement

Florian R. Steindl: Methodology, Formal analysis, Investigation, Data curation, Writing – original draft, Writing – review & editing. **Florian Mittermayr:** Methodology, Validation, Writing – review & editing, Funding acquisition. **Marlene Sakoparnig:** Investigation, Data curation, Writing – review & editing. **Joachim Juhart:** Validation, Writing – review & editing. **Lukas Briendl:** Investigation, Data curation, Writing – review & editing. **Benedikt Lindlar:** Investigation, Methodology, Writing – review & editing. **Neven Ukrainczyk:** Investigation, Methodology, Writing – review & editing. **Martin Dietzel:** Writing – review & editing, Supervision, Project administration. **Wolfgang Kusterle:** Writing – review & editing, Project administration, Funding acquisition. **Isabel Galan:** Conceptualization, Validation, Methodology, Writing – review & editing, Supervision, Project administration, Funding acquisition.

Declaration of Competing Interest

The authors declare that they have no known competing financial interests or personal relationships that could have appeared to influence the work reported in this paper.

Data availability

Data will be made available on request.

Acknowledgement

The authors gratefully acknowledge the help of Sonja Reitschmidt and Martin Peyerl of Smart Minerals GmbH in Vienna and Bernhard Marius of the Institute of Chemical Engineering and Environmental Technology of the Graz University of Technology for their support concerning mercury intrusion porosimetry and the operation of the instruments and Adrian Zimmermann of the Institute of Construction and Building Materials of the Technical University of Darmstadt for discussions concerning mercury intrusion porosimetry data analysis. Funding by the Austrian Research Promotion Agency FFG within the project ASSpC (Project-No. 856080) is thankfully acknowledged.

Appendix A. Supplementary data

Supplementary data to this article can be found online at https://doi.org/10.1016/j.conbuildmat.2023.130461, also containing a spreadsheet demonstrating the tool for pore size distribution analysis. This spreadsheet does already contain pore size distribution data, which can of course be exchanged for testing or application of the tool.

References

[1] P. Pipilikaki, M. Beazi-Katsioti, The assessment of porosity and pore size distribution of limestone Portland cement pastes, Constr. Build. Mater. 23 (2009) 1966–1970, https://doi.org/10.1016/j.conbuildmat.2008.08.028.
[2] V.T. Ngala, C.L. Page, Effects of carbonation on pore structure and diffusional properties of hydrated cement pastes, Cem. Concr. Res. 27 (1997) 995–1007, https://doi.org/10.1016/S0008-8846(97)00102-6.
[3] R. Kumar, B. Bhattacharjee, Porosity, Pore Size Distribution and In-situ Strength of Concrete, Cem. Concr. Res. 33 (2003) 155–164, https://doi.org/10.1016/S0008-8846(02)00942-0.
[4] N. Bossa, P. Chaurand, J. Vicente, D. Borschneck, C. Levard, O. Aguerre-Chariol, J. Rose, Micro- and nano-X-ray computed-tomography: A step forward in the characterization of the pore network of a leached cement paste, Cem. Concr. Res. 67 (2015) 138–147, https://doi.org/10.1016/j.cemconres.2014.08.007.
[5] J. Zhou, G. Ye, K. van Breugel, Characterization of pore structure in cement-based materials using pressurization–depressurization cycling mercury intrusion porosimetry (PDC-MIP), Cem. Concr. Res. 40 (2010) 1120–1128, https://doi.org/10.1016/j.cemconres.2010.02.011.
[6] M. Palacios, H. Kazemi-Kamyab, S. Mantellato, P. Bowen, Laser diffraction and gas adsorption techniques, in: K. Scrivener, R. Snellings, B. Lothenbach (Eds.), A Pract. Guid. to Microstruct. Anal. Cem. Mater., 1st ed., CRC Press, Boca Raton, 2016: pp. 445–483.
[7] G. De Schutter, K. Audenaert, Evaluation of water absorption of concrete as a measure for resistance against carbonation and chloride migration, Mater. Struct. 37 (2004) 591–596, https://doi.org/10.1617/14045.
[8] L. Bolduc, M. Jolin, B. Bissonnette, Evaluating the service life of shotcrete, CRC Press, Shotcrete, 2010, pp. 57–63, 10.1201/b10545-8.
[9] E. Berodier, J. Bizzozero, A.C.A. Muller, Mercury intrusion porosimetry, in: K. Scrivener, R. Snellings, B. Lothenbach (Eds.), A Pract. Guid. to Microstruct. Anal. Cem. Mater., 1st ed., CRC Press, Boca Raton, 2016: pp. 419–444.
[10] S. Diamond, Mercury porosimetry. An inappropriate method for the measurement of pore size distributions in cement-based materials, Cem. Concr. Res. 30 (2000) 1517–1525, https://doi.org/10.1016/S0008-8846(00)00370-7.
[11] K. Scrivener, R. Snellings, B. Lothenbach, A Practical Guide to Microstructural Analysis of Cementitious Materials, CRC Press (2018), https://doi.org/10.1201/b19074.
[12] I. Galan, A. Baldermann, W. Kusterle, M. Dietzel, F. Mittermayr, Durability of shotcrete for underground support– Review and update, Constr. Build. Mater. 202 (2019) 465–493, https://doi.org/10.1016/j.conbuildmat.2018.12.151.
[13] M. Sakoparnig, I. Galan, A. Balderman, F. Steindl, M. Dietzel, M. Thumann, A. Saxer, W. Kusterle, F. Mittermayr, Ca leaching of shotcrete & secondary precipitation - an experimental approach, in: J. Gemrich (Ed.), Proc. 15Th Int. Congr. Chem. Cem. (ICCC 2019), Research Institute of Binding Materials, Czech Republic, Prague, 2019, p. 2019.
[14] G. Bernardo, A. Guida, I. Mecca, Advancements in shotcrete technology, in: C.A. Brebbia, S. Hernandez (Eds.), Struct. Stud. Reparis Maint. Herit. Archit. XIV, WIT Trans. Built Environ. 153, 2015: pp. 591–602. https://doi.org/10.2495/STR150491.
[15] L.R. Prudêncio, Accelerating admixtures for shotcrete, Cem. Concr. Compos. 20 (2-3) (1998) 213–219.
[16] L.G. Briendl, F. Mittermayr, A. Baldermann, F.R. Steindl, M. Sakoparnig, I. Letofsky-Papst, I. Galan, Early hydration of cementitious systems accelerated by aluminium sulphate: Effect of fine limestone, Cem. Concr. Res. 134 (2020), 106069, https://doi.org/10.1016/j.cemconres.2020.106069.
[17] R.P. Salvador, S.H.P. Cavalaro, R. Monte, A.D. d. Figueiredo, Relation between chemical processes and mechanical properties of sprayed cementitious matrices containing accelerators, Cem. Concr. Compos. 79 (2017) 117–132, https://doi.org/10.1016/j.cemconcomp.2017.02.002.
[18] J. Armengaud, M. Cyr, G. Casaux-Ginestet, B. Husson, Durability of dry-mix shotcrete using supplementary cementitious materials, Constr. Build. Mater. 190 (2018) 1–12, https://doi.org/10.1016/j.conbuildmat.2018.09.107.
[19] I. Galan, L. Briendl, M. Thumann, F. Steindl, R. Röck, W. Kusterle, F. Mittermayr, Filler Effect in Shotcrete, Materials (Basel). 12 (2019) 3221, https://doi.org/10.3390/ma12193221.
[20] I. Galan, L. Briendl, M. Hoedl, F. Steindl, J. Juhart, F. Mittermayr, Early hydration of dry-mix sprayed concrete. Proc. 1St Int. Conf. Innov, Low-Carbon Cem. Concr. Technol, London, United Kingdom, 2019.
[21] L.G. Briendl, F. Mittermayr, R. Röck, F.R. Steindl, M. Sakoparnig, J. Juhart, F. Iranshahi, I. Galan, The hydration of fast setting spray binder versus (aluminum sulfate) accelerated OPC, Mater. Struct. 55 (2022), https://doi.org/10.1617/s11527-022-01907-x.
[22] M.R.M. Saade, A. Passer, F. Mittermayr, (Sprayed) concrete production in life cycle assessments: a systematic literature review, Int. J. Life Cycle Assess. 25 (2020) 188–207, https://doi.org/10.1007/s11367-019-01676-w.
[23] M. Romer, L. Holzer, M. Pfiffner, Swiss tunnel structures: concrete damage by formation of thaumasite, Cem. Concr. Compos. 25 (2003) 1111–1117, https://doi.org/10.1016/S0958-9465(03)00141-0.
[24] R.P. Salvador, D.A.S. Rambo, R.M. Bueno, S.R. Lima, A.D. Figueiredo, Influence of accelerator type and dosage on the durability of wet-mixed sprayed concrete against external sulfate attack, Constr. Build. Mater. 239 (2020), 117883, https://doi.org/10.1016/j.conbuildmat.2019.117883.
[25] P. Bamonte, P.G. Gambarova, A. Nafarieh, High-temperature behavior of structural and non-structural shotcretes, Cem. Concr. Compos. 73 (2016) 42–53, https://doi.org/10.1016/j.cemconcomp.2016.06.009.
[26] K. Bergmeister, Beton unter hohen Temperaturen – eine Frage der Tunnelsicherheit, Beton- Und Stahlbetonbau. 101 (2006) 74–80, https://doi.org/10.1002/best.200500467.
[27] J. Wang, D. Niu, S. Ding, Z. Mi, D. Luo, Microstructure, permeability and mechanical properties of accelerated shotcrete at different curing age, Constr. Build. Mater. 78 (2015) 203–216, https://doi.org/10.1016/j.conbuildmat.2014.12.111.
[28] B. Lagerblad, L. Fjällberg, C. Vogt, Shrinkage and durability of shotcrete, in: S. Bernard (Ed.), Shotcrete Elem. a Syst., CRC Press, 2010: pp. 173–180. http://www.diva-portal.org/smash/record.jsf?pid=diva2:496243.
[29] L. Fan, Z. Zhang, Y. Yu, P. Li, T. Cosgrove, Effect of elevated curing temperature on ceramsite concrete performance, Constr. Build. Mater. 153 (2017) 423–429, https://doi.org/10.1016/j.conbuildmat.2017.07.050.
[30] H. Li, D. Yan, G. Chen, S. Xu, J. Liu, Y. Hu, Porosity, pore size distribution and chloride permeability of shotcrete modified with nano particles at early age, J. Wuhan Univ. Technol. Mater. Sci. Ed. 31 (2016) 582–589, https://doi.org/10.1007/s11595-016-1413-9.

[31] M. Sakoparnig, G. Koraimann, L. Briendl, F. Steindl, T. Angerer, R. Lindlar, B., W. Kusterle, F. Mittermayr, Visualisierung und Untersuchung von Inhomogenitäten im Spritzbeton (Visualization and analysis of inhomogeneities in shotcrete)., in: W. Kusterle (Ed.), Spritzbeton-Tagung 2021, Alpbach, Austria. (submitted), 2021.
[32] F.R. Steindl, F. Mittermayr, M. Thumann, J. Juhart, I. Galan, A. Baldermann, L. Briendl, M. Sakoparnig, R. Röck, W. Kusterle, Sulfate resistance of dry mix shotcretes with new binder composition, in: J. Gemrich (Ed.), Proc. 15Th Int. Congr. Chem. Cem. (ICCC 2019), Research Institute of Binding Materials, Prague, Czech Republic, 2019.
[33] Austrian Society for Construction Technology (öbv), Sprayed Concrete Guideline, Österreichische Vereinigung für Beton- und Bautechnik, Vienna, 2013.
[34] F.R. Steindl, I. Galan, A. Baldermann, M. Sakoparnig, L. Briendl, J. Juhart, M. Thumann, M. Dietzel, R. Röck, W. Kusterle, F. Mittermayr, Sulfate durability and leaching behaviour of dry- and wet-mix shotcrete mixes, Cem. Concr. Res. 137 (2020), 106180, https://doi.org/10.1016/j.cemconres.2020.106180.
[35] R.P. Salvador, S.H.P. Cavalaro, Á. Rueda, A.D. De Figueiredo, Hydration and Microstructure Development in Accelerated Cement Pastes Produced by Spraying for the Evaluation of Shotcrete, 14th Int, Congr. Chem. Cem. (2015) 1–7. http://www.iccc2015beijing.org/dct/page/1.
[36] D. Lootens, B. Lindlar, R.J. Flatt, Some peculiar aspects of shotcrete accelerators, in: W. Sun, K. van Breugel, C. Miao, G. Ye, H. Chen (Eds.), Int. Conf. Microstruct. Relat. Durab. Cem. Compos., 2008: pp. 1255–1261.
[37] Austrian Standards Institute, ÖNORM B 3309-1. Processed hydraulic additions for concrete production - Part 1: Combination products., Austrian Standards Institute, Vienna, 2010.
[38] I. Galan, M. Thumann, L. Briendl, R. Röck, F. Steindl, J. Juhart, F. Mittermayr, W. Kusterle, From Lab Scale Spraying to Real Scale Shotcreting and Back to the Lab, in: T. Beck, S.A. Myren, S. Engen (Eds.), Proc, 8th Int., Symp, Sprayed Concr., Trondheim, Norway, 2018.
[39] B. Lindlar, C. Stenger, D. Lootens, Miniaturisiertes Laborspritzverfahren für Spritzbeton - Neue Möglichkeiten der Produktentwicklung, Rezepturoptimierung und Qualitätskontrolle. Miniaturised laboratory spray method for shotcrete - new possibilites for the product development, mix design op, in: W. Kusterle (Ed.), Spritzbeton-Tagung 2015, Alpbach, Austria, 2015.
[40] I. Galan, H. Beltagui, M. García-Maté, F.P. Glasser, M.S. Imbabi, Impact of drying on pore structures in ettringite-rich cements, Cem. Concr. Res. 84 (2016) 85–94, https://doi.org/10.1016/j.cemconres.2016.03.003.
[41] R.A. Cook, K.C. Hover, Experiments on the contact angle between mercury and hardened cement paste, Cem. Concr. Res. 21 (1991) 1165–1175, https://doi.org/10.1016/0008-8846(91)90077-U.
[42] M.R. Rezaee, A. Jafari, E. Kazemzadeh, Relationships between permeability, porosity and pore throat size in carbonate rocks using regression analysis and neural networks, J. Geophys. Eng. 3 (2006) 370–376, https://doi.org/10.1088/1742-2132/3/4/008.
[43] Z. Gao, Q. Hu, Estimating permeability using median pore-throat radius obtained from mercury intrusion porosimetry, J. Geophys. Eng. 10 (2) (2013) 025014.
[44] J. Juhart, L. Briendl, F. Mittermayr, M. Thumann, R. Röck, W. Kusterle, Optimierte Eigenschaften von Spritzbeton durch kombinierte Zusatzstoffe, in: W. Kusterle (Ed.), Spritzbet, Tagung 2018, Alpbach, 2018, pp. 1–20.
[45] J. Juhart, G.-A. David, M.R.M. Saade, C. Baldermann, A. Passer, F. Mittermayr, Functional and environmental performance optimization of Portland cement-based materials by combined mineral fillers, Cem. Concr. Res. 122 (2019) 157–178, https://doi.org/10.1016/j.cemconres.2019.05.001.
[46] C. Herrera-Mesen, R.P. Salvador, T. Ikumi, S.H.P. Cavalaro, A. Aguado, External sulphate attack of sprayed mortars with sulphate-resisting cement: Influence of accelerator and age of exposition, Cem. Concr. Compos. 114 (2020), 103614, https://doi.org/10.1016/j.cemconcomp.2020.103614.
[47] S.T. Lee, D.G. Kim, H.S. Jung, Sulfate attack of cement matrix containing inorganic alkali-free accelerator, KSCE J. Civ. Eng. 13 (2009) 49–54, https://doi.org/10.1007/s12205-009-0049-0.
[48] R.P. Salvador, S.H.P. Cavalaro, M. Cano, A.D. Figueiredo, Influence of spraying on the early hydration of accelerated cement pastes, Cem. Concr. Res. 89 (2016) 187–199, https://doi.org/10.1016/j.cemconres.2016.07.015.
[49] L.G. Briendl, C. Grengg, B. Müller, G. Koraimann, F. Mittermayr, P. Steiner, I. Galan, In situ pH monitoring in accelerated cement pastes, Cem. Concr. Res. 157 (2022), 106808, https://doi.org/10.1016/j.cemconres.2022.106808.
[50] M. Sakoparnig, I. Galan, W. Kusterle, B. Lindlar, G. Koraimann, T. Angerer, F. R. Steindl, L.G. Briendl, S. Jehle, J. Flotzinger, J. Juhart, F. Mittermayr, On the significance of accelerator enriched layers in wet-mix shotcrete, Tunn. Undergr. Sp. Technol. 131 (2023), 104764, https://doi.org/10.1016/j.tust.2022.104764.